

Towards a new (Q, t) regime by time-resolved X-ray diffraction: Ultra-sound excited crystals as an example

K. D. LISS¹(*), A. MAGERL², R. HOCK³, A. REMHOF⁴ and B. WAIBEL^{2,4}

¹ *European Synchrotron Radiation Facility - F-38043 Grenoble Cedex, France*

² *Institut Max von Laue Paul Langevin - F-38042 Grenoble Cedex, France*

³ *Institut für Mineralogie der Universität Würzburg*

Am Hubland, D-97074 Würzburg, Germany

⁴ *Institut für Experimentalphysik 4, Ruhr Universität Bochum*

D-44780 Bochum, Germany

(received 28 July 1997; accepted 2 October 1997)

PACS. 07.85Qe – Synchrotron radiation instrumentation.

PACS. 61.20Lc – Time-dependent properties; relaxation.

PACS. 43.35+d – Ultrasonics, quantum acoustics, and physical effects of sound.

Abstract. – Time-resolved diffraction patterns down to a sub-nanosecond scale obtained with a high-resolution diffractometer for high-energies X-rays on ultrasonically excited samples are presented. The time resolution gives direct insight into the purity of the excited sound waves and reveals the density of states for the lattice parameter at any point of time in a MHz oscillation period. The combination of the time resolution with the momentum transfer Q accessible by the high-energy diffractometer gives access to a unique regime in (Q, t) space.

Diffraction in perfect single crystals is described by the theory of dynamical diffraction. This approach considers the complete wave pattern propagating in the periodic potential of an ideal crystal, and a rich variety of phenomena like Pendellösung oscillations, rapid intensity variations within the Borrmann fan, or anomalous transmission of X-rays is explained. All these features are described quantitatively from the interference patterns of the wave fields in the crystal and the appropriate boundary conditions at the crystal surface. One of the most important effects of dynamical diffraction is the strongly limited intensity diffracted by an ideal crystal in Bragg position. The interference effects from the wave fields disappear very quickly if the perfect translational symmetry in a crystal is violated due to any disturbance. Simultaneously, the Bragg-reflected intensity increases rapidly in this case. A pure mode ultrasonic wave is a simple and well-defined disturbance of the crystal lattice and allows to study the transition in diffraction from a perfect crystal reflecting a weak intensity towards an imperfect crystal diffracting an enlarged wavelength band. The degree of crystal imperfection is easily controlled by the sound wave amplitude. On this background several studies have

(*) E-Mail: liss@esrf.fr

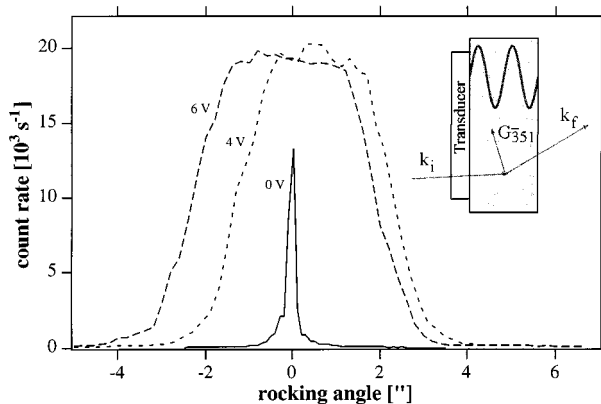


Fig. 1. – Rocking curves of 100 keV X-radiation Bragg diffracted on the Si $\bar{3}51$ reflection for three different excitation voltage parameters of a 2.353 MHz sound wave. The inset sketches the crystal with the scattering vector and the longitudinal sound wave in the [111] direction.

been conducted recently with the aim to develop improved optical elements for synchrotron X-ray [1], [2] and neutron diffraction [3], [4].

So far measurements at ultrasound frequencies in the MHz range have given information reflecting time-averaged distortions in the crystal, whereas no information can be obtained on momentary strains relating to the phase of the sound excitation. *E.g.*, high-resolution rocking scans are shown in fig. 1. The diffraction geometry used is illustrated as an inset. Note that for this arrangement the X-ray beam passes through the entire silicon sample with a thickness of 10 mm. Because typical sound wavelengths in our setup are 0.5 mm, the diffraction pattern takes a spatial average over the entire distortion pattern of the sound wave. Figure 1 presents a high-resolution rocking curve of the $\bar{3}51$ Bragg peak without and with ultra-sound excitation at various levels. The data were taken with synchrotron radiation of 100 keV at the high energy beamline ID15A at the ESRF (European Synchrotron Radiation Facility). At this X-ray energy attenuation becomes small and can be neglected even for our silicon crystal with a thickness of 10 mm. Further experimental details are given in [1]-[5]. Figure 1 demonstrates the strong increase in the Bragg intensity on sound excitation. This enhancement relates to a purely longitudinal character of the crystal deformation along the 111 direction of the sound wave. In addition, the largest rocking width of the Bragg peak corresponds to a peak-to-peak amplitude of the acoustic wave reaching 900 Å in fig. 3 c). As already referred to, the information obtained in such spectra is averaged over the period of the sound wave.

In the present investigation we add a new dimension to diffraction scans on ultra-sound excited crystals by associating a time resolution sufficiently rapid such that the measurements becomes sensitive to the crystal response as a function of the temporal phase of an ultra-sound wave in the MHz range.

A commercial germanium crystal detector about 30 mm thick and with intrinsic conductivity was employed in the experiment. The material and the dimension were optimized for the high-energy radiation used. Since the scattering process is instantaneous, two kinds of time determination can be envisaged. First, the detector itself resolves the time when the diffraction takes place. The leading edge of the charge signal after the detector preamplifier has a rise time of 100 ns. The electronic signal can be shaped by a discriminator system and a time resolution of 20 ns full width at half-maximum (FWHM) is achieved in this way. A

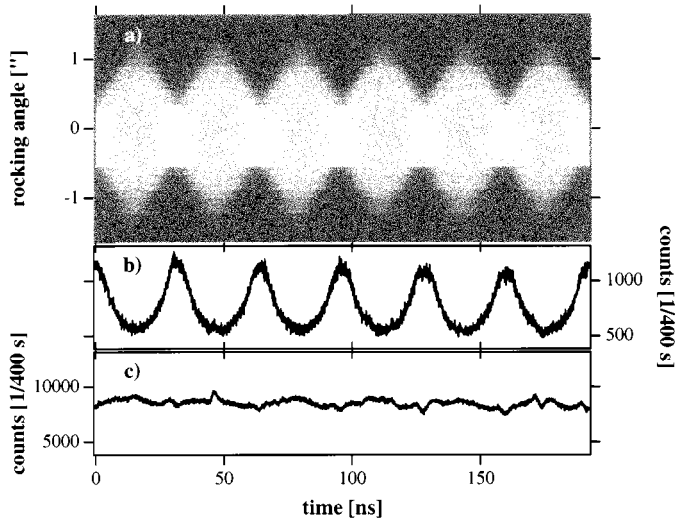


Fig. 2. – Intensity distribution in the rocking-angle time coordinate plane (a), a section through the center of the rocking curve (b) and the integrated intensity (c) developing in time. The excitation frequency is 15.5991 MHz.

coincidence with the slower energy-discriminated signal ensures that only photons with the right energy and thus the right trigger point are registered. This method is independent of the time structure of the electron bunches in the storage ring of the synchrotron. Alternatively, the time resolution can be improved further by taking advantage of the pulse width of a single-electron bunch in the synchrotron storage ring. In the 16 bunch mode of operation at the ESRF storage ring individual light bursts are separated by 176 ns, whereas an individual bunch emits radiation towards an experimental station for less than 100 ps [6]. Thus, by a coincidence method relating the counts and the bunch structure it seems possible to attribute an individual event to a particular bunch with a time resolution of 100 ps —although the detector system has a significantly poorer time response. In both modes of operation a fast multi-channel analyzer was triggered whenever a signal was detected. The stop signal was derived from the zero-amplitude condition of the sound generator. Since photon events are rare as compared to the trigger signals occurring at a MHz frequency, saturation of the counting chain is avoided in this mode of start/stop signals. Using the time structure of a single bunch of the synchrotron with an intrinsic width of less than 0.1 ns the total time resolution of our detector system was calibrated to be 20 ns FWHM in the first and 0.2 ns in the second set up. During data acquisition the intensity is stroboscopically accumulated over a few minutes counting time while the sample is kept at appropriate rocking angles.

A time-resolved diffraction scan taken with the 0.2 ns resolution at a photon energy of 258 keV is displayed in fig. 2. It shows the time evolution of the Bragg intensity for a pure mode standing wave with a frequency of 15.5991 MHz. Within one oscillation period of 64 ns there are two well-defined diffraction maxima with a rocking width extending out to $1.6''$ FWHM. Positive and negative rocking angles in fig. 2 a) correspond to compressed and expanded lattice spacings, respectively. Intensities diffracted from compressed and expanded regions of the crystal appear simultaneously because of the scattering geometry by which a spatial average over the entire crystal thickness is performed. The minimum rocking width is $0.8''$ which still is larger than the ideal crystals rocking width of $0.2''$. Nevertheless, these

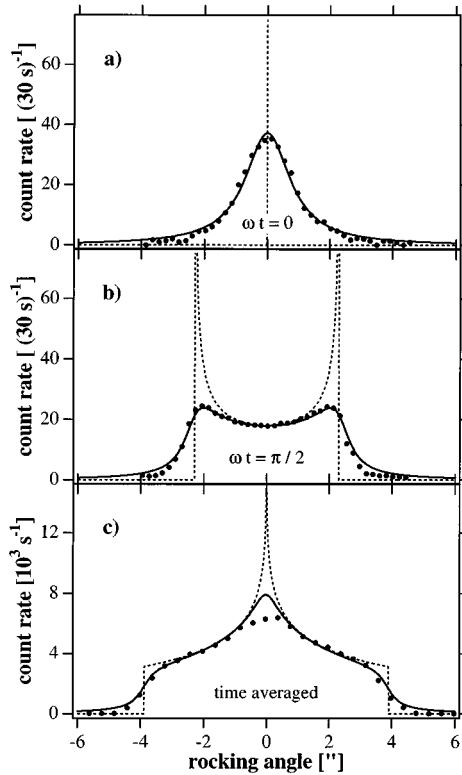


Fig. 3. – Snapshots for an excited crystal at moments where the lattice is mostly relaxed and at maximum strain given by the large dots in a) and b), respectively. Plot c) gives time-averaged data obtained without any timing setup. All three curves follow well the behavior predicted by the theory, a Dirac delta-function in a), an inverse circle function in b) and a complete elliptic integral of the first kind in c). The theoretical distributions are given by the dotted lines whereas the continuous lines in b) and c) are folded with the same Lorentzian resolution function.

data resolve the moments in time when the entire crystal is largely relaxed or when it is at its maximum mechanical load. Figure 2 b) shows the section through the center of the rocking curve. It clearly demonstrates that the intensity peaks when the rocking curve is narrowest. The angular integrated intensity displayed in fig. 2 c) shows a nearly constant value for an entire sound period. Since it does not depend on the strain distribution, it indicates that the crystal behaves like a kinematical scatterer. A similar scan has been taken at 300 keV with an ultra-sound frequency of 8.1792 MHz and in the 20 ns time resolution mode [7]. Snapshots of the rocking curve at moments of minimal and maximal strain are given in figs. 3 a) and b), their rocking widths corresponding to 2.0'' and 5.3'', respectively. The curve in fig. 3 a) fits well to a Lorentzian, the diffraction profile of a strain free crystal in Laue geometry. Nevertheless, it is enlarged due to the finite time resolution which is 16% of the full oscillation period and still too coarse to observe the sharp moment of complete strain relaxation. The snapshot in fig. 3 b) shows two maxima at the extremes and a minimum in the center of the reflection curve depicting the density of states for the lattice parameters at the moment of maximum strain induced by the ultrasound.

Let

$$u(x) = u_0 \sin(\omega t) \sin(kx) \quad (1)$$

describe a longitudinal standing wave of the displacement of atoms at position x and time t , u_0 , $\omega/2\pi$ and k representing maximal wave amplitude, frequency and the wave number, respectively. The probability $\rho(u)$ to find a particular amplitude at given time somewhere in the crystal is given by the derivative of the inverse function, *i.e.*

$$\rho(u) = \frac{\partial x}{\partial u} = \frac{1}{k\sqrt{u_t^2 - u^2}}, \quad (2)$$

with $u_t = u_0 \sin(\omega t)$. The denominator describes an arc of a circle and (2) is called the inverse circle function. It has integrable poles at the maximum amplitude u_t and a local minimum with a final value in the center. Such a distribution is given by the dotted line in fig. 3 b). Folded with a Lorentzian resolution function of 0.8'' FWHM, the fitted continuous line results. The data shows well the sharp rising edges and the dip in the center. A time-averaged scan at 100 keV and 2.55764 MHz is given in fig. 3 c). For its interpretation one has to average the distribution (2) over one oscillation period, *i.e.*

$$\bar{\rho}(u) = \frac{2\omega}{\pi} \int_0^{\frac{\pi}{2\omega}} \rho(u) dt = \frac{2}{\pi k} \int_u^{u_0} \frac{du_t}{\sqrt{(u_t^2 - u^2)(u_0^2 - u_t^2)}} = \frac{2}{\pi k u_0} K \left(\sqrt{1 - \frac{u^2}{u_0^2}} \right). \quad (3)$$

$K(q)$ is the complete elliptic integral of the first kind with modulus q [8]. This function, illustrated by the dashed line in fig. 3 c), shows a discontinuity at the maximum of the amplitude's absolute value and then a concave increase to the integrable logarithmic pole in the center. Again, we convoluted this function with the same resolution as above to obtain the continuous line which fits well to the data. We note, in particular, that the data show a rapid increase forming the shoulder at $\pm 3.5''$ followed by a further progressive augmentation towards the center.

The salient feature of the time-resolved scans refer to the fact that the momentary states of the strain distribution become accessible. First results using this technique taught that it is quite unlikely to obtain a clean standing wave mode as displayed in fig. 2. Instead, a distribution of harmonics is usually excited breaking the symmetry of the diffraction pattern in rocking angle at a given moment. Apart from possible extinction effects this explains why most time-averaged rocking scans, see fig. 1 and ref. [1], do not reveal the shape of the distribution (3). Pure sound modes can be best obtained by exciting the eigenresonances of the sample crystal at frequencies far enough off the transducer resonance. Then the transducer amplitude is small but the resonance effect amplifies the atomic displacements in the sample resulting in large rocking widths related directly to the sound amplitude u_0 . The reduced rocking width would have become apparent in a traditional time-averaged measurement. However, the reason for the reduced reflectivity would not be obvious. In contrast, time-resolved diffraction patterns of high-energy synchrotron radiation provide a unique possibility to evaluate the quality of the excited mode and to access details of the distortions in the bulk of a crystal. Thus the time-resolved data allow us to determine for any phase the characteristics of the crystal deformation induced by a sound wave. Eventually, it should be possible to study properties like anharmonocities at any phase of the wave.

To put things into their perspective, we emphasize that we reported in this paper on a measurement of the structural response of a crystal to an ultra-sound excitation, and the technique exposed allows to follow this response with a time resolution of 0.2 ns. However, the disturbance needs not to be limited to ultra-sound. Any excitation can be considered

which results in an atomic displacement and which manifests itself by a modification of the intensity of a Bragg peak. The relaxation of this change of the Bragg scattering towards its equilibrium value can be followed with the same time resolution. Although some time resolved experiments on the ns scale have been reported earlier [9]-[11], intense high-energy X-ray beams now available at synchrotron sources add a particular benefit to such studies. First, the high penetration power does away with surface problems and many limitations of the sample environments such that true bulk properties can be studied. A second advantage of high-energy X-rays, which likely is more important, concerns the large volume of reciprocal space up to a momentum transfer Q of some 30 \AA^{-1} becoming accessible. In this way Bragg reflections can be chosen with a structure factor which is particularly sensitive to a specific displacement pattern. This potentially can enhance the sensitivity of the technique to look into fine details of atomic or molecular motions. Actual and future trends concerning time-resolved X-ray diffraction are reviewed in the literature [11] revealing only a few examples of potential applications related to dynamics in solid-state physics, biology and chemistry.

REFERENCES

- [1] LISS K.-D., MAGERL A., REMHOF A. and HOCK R., *Acta Crystallogr. A*, **53** (1997) 181.
- [2] POLIKARPOV I. V., PANOV V. and BARTUNIK H. D., *J. Appl. Crystallogr.*, **27** (1994) 453.
- [3] HOCK R., VOGT T., KULDA J., MURSIC Z., FUESS H. and MAGERL A., *Z. Phys. B*, **90** (1993) 143.
- [4] REMHOF A., LIß K.-D. and MAGERL A., *Nucl. Instrum. Methods A*, **391** (1997) 485.
- [5] LISS K.-D., ROYER A., TSCHENTSCHER T., SUORTTI P. and WILLIAMS A. P., *On high resolution reciprocal space mapping with a triple crystal diffractometer for high energy X-rays*, to be published in *J. Synchrotron Radiation*, (1997).
- [6] REVOL J.-L., PLOUVIEZ E. and RÜFFER R., *Synchrotron Radiation News*, **7** (4) (1994) 23.
- [7] LISS K.-D., MAGERL A., HOCK R. and REMHOF A., *The evolution of an ultrasonic strain field followed by diffraction with a 20 ns time resolution*, in *ESRF highlights*, (1996), p. 46-47. Or <http://www.esrf.fr/highlights/Science/Mater.htm#mat5>.
- [8] GRADSHTEYN I. S. and RYZHIK I. M., *Table of integrals, series, and products* (Academic Press, New York) 1980.
- [9] KIKUTA S., TAKAHASHI T. and NAKATANI S., *Jpn. J. Appl. Phys.*, **23** (4) (1984) L193.
- [10] FOLLATH R. and JEX H., *Physica Status Solidi B*, **182** (1994) 485.
- [11] WARK J., *Contemp. Phys.*, **37** (3) (1996) 205.